JOURNAL OF SOLID STATE CHEMISTRY 89, 345–360 (1990)

Magnetism, Superconductivity, and the Metal–Nonmetal Transition in the Spinel $LiM_xTi_{2-x}O_4$; $M = Al^{3+}, Cr^{3+}$

P. M. LAMBERT*

Baker Laboratory of Chemistry, Cornell University, Ithaca, New York 14853

P. P. EDWARDS†

University Chemical Laboratory, Lensfield Road Cambridge CB2 1EW, and Interdisciplinary Research Centre in Superconductivity, University of Cambridge, Madingley Road, Cambridge, United Kingdom

AND M. R. HARRISON

GEC Hirst Research Centre, East Lane, Wembley, Middlesex HA9 7PP, United Kingdom

Received June 2, 1988; in revised form July 24, 1990

In the $LiM_xTi_{2-x}O_4$ ($M = Cr^{3+}, Al^{3+}$) spinel solid solution systems, the M^{3+} cations substitute at the octahedral sites and thus directly interact with the titanium 3*d* conduction electrons. The effect is dramatically illustrated in the chromium series where superconductivity is supressed completely at 2.5% Cr^{3+} substitution by a magnetic impurity effect. Infrared transmission measurements indicate a metal–nonmetal transition (MNMT) in $LiCr_xTi_{2-x}O_4$ at $0.33 < x < 0.40$. In the aluminum series, the superconducting transition temperature T_c persists at a high value (> 6 K) to $x = 0.33$, where a MNMT is proposed. Percolation, disproportionation, and conduction electron concentration are briefly discussed as possible contributing mechanisms for the MNMT in the cation-substituted $LiM_xTi_{2-x}O_4$ ($M = Li^+, Al^{3+}, Cr^{3+}$) system.

Introduction

The metallic spinel $LiTi_2O_4$ was originally synthesized and structurally characterized by Deschanvres *et al.* (*1*) as an endmember in the $Li_{1+x}Ti_{2-x}O_4$ ($0 \le x \le 1/3$) solid solution series. Johnston subsequently found $LiTi_2O_4$ to be a high temperature superconductor with $T_c = 11$ K (*2, 3*). Interestingly, all metallic compositions in the $Li_{1+x}Ti_{2-x}O_4$ series are superconducting with nearly the same transition temperature (*4–6*).

X-ray diffraction studies (*1, 3, 5*) show that $LiTi_2O_4$ possesses a normal spinel cation distribution; the lithium cations are located at the tetrahedral sites and the titanium cations occupy the octahedral sites. In the $Li_{1+x}Ti_{2-x}$ series, the additional lithium cations randomly substitute on the spinel octahedral sites as x increases, while the titanium cations remain restricted to the octahedral sublattice. The metallic character of $LiTi_2O_4$ is thus derived from direct tita-

*Present address: Eastman Kodak Co, Diversified Technologies Group, Research Laboratories, Rochester, New York 14650, USA.

†To whom correspondence should be addressed.

0022-4596/90 $3.00

nium 3*d* orbital overlap between adjacent, edge-sharing octahedra. A conduction band composed largely of titanium 3*d* t_{2g} orbitals is approximately 1/12 filled in $LiTi_2O_4$.

In an effort to better understand the $Li_{1+x}Ti_{2-x}O_4$ system, we have studied the structural, magnetic, and electronic effects of Mn^{2+} and Mg^{2+} substitution at the tetrahedral sites in $LiTi_2O_4$ (*7*). In the present work, we report the results of Cr^{3+} and Al^{3+} substitution in the octahedral sublattice of the same parent compound and present a comparison of the physical properties and the composition-induced metal–nonmetal transitions of the $LiM_xTi_{2-x}O_4$ systems (M = Li^+, Cr^{3+}, Al^{3+}).

Experimental

Stoichiometric amounts of Li_2CO_3 (Atomergic, 99.99%), TiO_2 (AESAR, 99.998% Puratronic), Ti_2O_3, and either Cr_2O_3 (AESAR, 99.99% Puratronic) or Al_2O_3 (AESAR, 99.99% Puratronic) were combined and fired in a two-step process according to the overall reaction scheme,

$$Li_2CO_3 + 2TiO_2 + (1 - x)Ti_2O_3 + xM_2O_3 \rightarrow 2LiM_xTi_{2-x}O_4 + CO_2, \quad (1)$$

where M is Cr^{3+} or Al^{3+}. The Ti_2O_3 was prepared from Ti metal (AESAR, 99.99%) and TiO_2 at 1600°C under RF heating in vacuum. The starting materials were dried and checked for phase purity by X-ray diffraction.

After mixing and pelletizing, the air stable components were fired at 750°C in air for 2.5 hr. The requisite amount of Ti_2O_3 was then mixed with the prefired material and pelletized. The pellets were wrapped in 0.001 in. OFHC Cu foil and sealed in evacuated quartz tubes for the final firing. The firing temperatures varied linearly with x from 850°C (x = 0.0) to 1000°C (for x = 0.0) for 18 hr and then allowed to furnace cool to ambient temperature. Additional preparative details have been described earlier (*7*, *8*).

X-ray powder diffraction patterns were obtained for all samples with 114.6-mm diameter Debye–Scherrer cameras using Ni-filtered Cu$K\alpha$ radiation. Powder diffraction tracings were obtained with an Enraf-Nonius diffractometer equipped with a Stoe Bragg-Brentano goniometer (NRC Laboratory, Ottawa, Canada).

The normalized integrated peak intensities obtained from the diffractometer tracings were used to determine u, the crystallographic spinel oxygen parameter, and the cation site distribution in several samples. The Furuhashi method (*9*) was used for the above analysis, with theoretical intensities determined by the LAZY PULVERIX program (*10*). A heuristic search in the u and cation distribution space located the most probable structure (*7*).

Static magnetic susceptibility measurements were obtained on the computer-interfaced Faraday balance (*11*). Calibration was performed using $HgCo(SCN)_4$ as a standard.

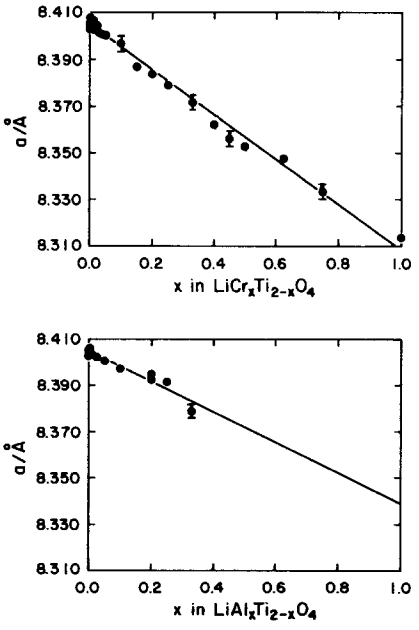

FIG. 1. The compositional dependence of the lattice parameter (a) in $LiCr_xTi_{2-x}O_4$ and (b) in $LiAl_xTi_{2-x}O_4$.

The temperature-independent Van Vleck paramagnetism of Ti^{4+} in an octahedral oxygen environment (*12, 13*) approximately compensates for the core diamagnetism in all samples, and so core corrections were not applied to the susceptibilities.

Superconducting transition temperatures were measured on an AC inductance instrument operating at 400 Hz (*11*). Transition temperatures are reported at 50% of full signal deflection and transition widths as between 10% and 90% deflection.

Infrared transmission measurements were obtained on either a Perkin–Elmer 337 grating infrared spectrophotometer from 1333 to 444 cm^{-1} or an IBM FTIR spectrophotometer (Series IR/90) from 1000 to 400 cm^{-1}. Samples were prepared as pellets using the KBr technique.

Structural Parameters

Single-phase powder samples of the $LiCr_xTi_{2-x}O_4$ series were prepared for $0 < x < 1$. A distinctive color change occurs as the chromium concentration is increased; the blue color of $LiTi_2O_4$ changes to a green color in the intermediate x value compositions and gradually becomes orange-brown in $LiCrTiO_4$. All diffraction lines were indexed to a cubic system consistent with the spinel unit cell. The lattice parameters (a) for the chromium series (Fig. 1) obey Vegard's law. The lattice parameter of $LiCrTiO_4$, $a = 8.3135(8)$ Å, is in excellent agreement with the literature values of 8.31 Å (*14*) and 8.32 Å (*15*).

Compositions of the $LiAl_xTi_{2-x}O_4$ series were prepared as predominately single-phase spinels up to $x = 0.25$. The $x = 0.33$ sample originally contained $LiAl_5O_8$ as an impurity. However, refiring the sample at 915°C for 2 hr removed the majority of this phase leaving only the spinel phase and a trace of the unidentified impurity phase observed by Inukai and Murakami (*16*) and Harrison *et al.* (*6*). Refiring at higher temperature gave a mixture of spinel and ramsdellite phases (*17*). At higher x values, in addition to the cubic phase, substantial amounts of both impurities were observed, depending on the firing and refiring temperatures; measurements are reported only for compositions up to $x = 0.33$.

The lattice parameters for the aluminum series (Fig. 1) show a linear dependence with composition (within experimental error) through the $x = 0.33$ sample. The color of the compounds changes as x increases from blue to grey-white at $x = 0.33$. This trend resembles the color changes observed in the $Li_{1+x}Ti_{2-x}O_4$ series, and is one of many similarities between the systems.

Blasse (*18*) claimed to have prepared single-phase $LiAlTiO_4$ by firing Li_2CO_3, TiO_2, and Al_2O_3 in a 1 : 1 CO_2/O_2 atmosphere at 1000°C for 24 hr. Two different lattice parameters are reported, $a = 8.30$ Å (*15*) and $a = 8.34$ Å (*18*). In our investigation, a duplication of the conditions described above gave a multiphased product. Kordes and Rottig (*14*) attempted the preparation of $LiAlTiO_4$ and reported only a noncubic phase as a product.

Qualitative cation site distributions for the members of the $LiM_xTi_{2-x}O_4$ systems are easily obtained since, in the spinel structure, diffraction lines with the restrictions

$$hkl: \quad \begin{matrix} h \neq 2n+1 \\ k \neq 2n+1 \\ l = 2n+1 \end{matrix} \quad \text{or} \quad \begin{matrix} 4n+1 \\ 4n+1 \\ 4n+1 \end{matrix} \quad \text{or} \quad \begin{matrix} 4n \\ 4n \\ 4n \end{matrix} \quad \text{and} \quad h+k+l = 4n \qquad (2)$$

are almost totally dependent upon the atomic form factor of the cations occupying the tetrahedral sites. With lithium at the tetrahedral position, the intensity of these diffraction lines is nearly zero, and any significant substitution of a cation with a higher

TABLE I

CATION SITE DISTRIBUTIONS FOR $LiM_xTi_{2-x}O_4$

Composition	Best fit	ln K	u	B_{eff}
x = 0.00	$Li_{0.95}[Ti_2]O_4$	0.470	0.2600	0.684
Al x = 0.25	$Li[Al_{0.25}Ti_{1.75}]O_4$	−0.0154	0.2617	1.128
Cr x = 0.33	$Li_{0.97}Ti_{0.03}[Cr_{0.33}Ti_{1.64}]O_4$	0.0620	0.2620	1.095
Cr x = 0.625	$Li[Cr_{0.625}Ti_{1.375}]O_4$	0.0178	0.2623	0.671
Cr x = 1.00	$Li[CrTi]O_4$	0.0426	0.2620	0.421

Note. K is scale factor. B_{eff} is effective temperature factor.

atomic form factor (e.g., Al^{3+},Cr^{3+}) produces an observable line intensity. In all the $LiM_xTi_{2-x}O_4$ samples prepared little, if any, tetrahedral line intensity is apparent in the X-ray powder patterns.

These qualitative observations are substantiated by X-ray line intensity analysis (Table I) using the Furuhashi method (*9*). The most reasonable cation distribution is considered to be that which gives the best linearity for the relation

$$\ln(I_{obs}/I_{calc}) = \ln K - 2\beta_{eff}(\sin 2\Theta/\lambda 2), \quad (3)$$

where K is a scale factor, β is the effective temperature factor, λ is the X-ray wavelength and,

$$I_{calc} = |FF^*| Lpm \quad (4)$$

where F is the calculated structure factor, L is the Lorentz factor, p is the polarization factor, and m is the multiplicity of the reflection. Each composition is close to the desired cation distribution of $Li[M_xTi_{2-x}]O_4$, where the brackets indicate octahedral coordination.The u parameter of 0.262 for $LiCrTiO_4$ is close to the reported value of 0.260 (*15*).Theoretical and observed intensities are compiled in Table II for x = 0.33, 0.625, and 1.00 of the $LiCr_xTi_{2-x}O_4$ series and x = 0.25 of the $LiAl_xTi_{2-x}O_4$ series.

Superconductivity

The superconducting transition temperature declines sharply with increasing x in the $LiCr_xTi_{2-x}O_4$ series (Fig. 2), until by x = 0.05 (2.5% titanium substitution) the transition can no longer be detected. At lower x values, T_c falls linearly from 10 K at x = 0.0 to ≈4.6 K at x = 0.04. Such rapid diminution is not unexpected since Cr^{3+}, with three unpaired d electrons, should produce a strong magnetic impurity effect.

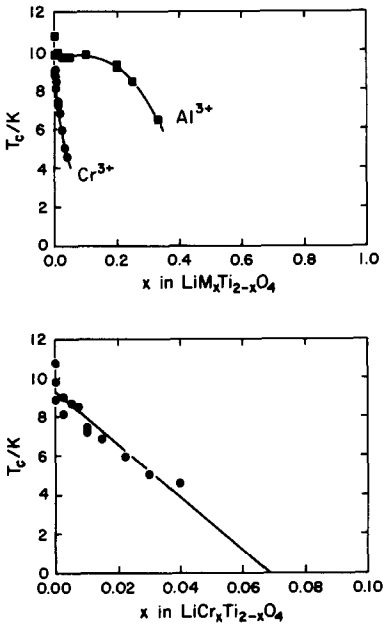

FIG. 2. Superconducting transition temperatures, T_c versus x for $LiM_xTi_{2-x}O_4$. The bottom figure is an expanded version of the data for $LiCr_xTi_{2-x}O_4$ ($0 < x < 0.05$).

The Abrikosov–Gor'kov relation (*19*) describes to first order the magnetic impurity effect and reduces to the linearly asymptotic form

$$T_c/T_{c0} = 1 - 0.691(n/n_{cr}) \quad (5)$$

as n tends toward zero, where T_{c0} is the transition temperature of the undoped host material, and n_{cr} is the critical electron concentration for the complete loss of superconductivity. Thus, the transition temperature falls nearly linearly with n and hence x to approximately T_c/T_{c0} = 0.45 (*20*).

Within experimental error, the chromium system displays similar behavior, as shown in Fig. 2. The T_c data for the higher x values should be considered to be less reliable be-

TABLE II

THEORETICAL AND OBSERVED X-RAY INTENSITIES FOR $LiAl_{0.25}Ti_{1.75}O_4$, $LiCr_{0.33}Ti_{1.67}O_4$, $LiCr_{0.625}Ti_{1.375}O_4$ AND $LiCrTiO_4$

	$LiAl_{0.25}Ti_{1.75}O_4$		$LiCr_{0.33}Ti_{1.67}O_4$		$LiCr_{0.625}Ti_{1.375}O_4$		$LiCrTiO_4$	
hkl	Observed	Calculated	Observed	Calculated	Observed	Calculated	Observed	Calculated
111	1000	1000	1000	1000	1000	1000	1000	1000
220	6	7	—	—	7	6	11	6
311	468	433	472	466	460	444	496	454
222	31	45	48	61	56	68	70	75
400	616	574	642	560	597	558	609	567
331	65	75	89	77	85	83	95	89
511 + 333	188	173	199	181	195	190	210	187
440	331	303	342	304	321	306	326	319
531	106	103	110	103	128	112	125	119
533	40	35	43	37	31	38	41	41
622	31	30	35	34	38	39	50	43
444	69	69	68	65	74	71	75	77
711 + 551	44	50	53	49	61	56	58	60
731 + 531	41	51	60	51	59	55	58	61
800	26	34	25	33	33	36	48	41

cause of a decrease in signal amplitude. This indicates that less of the sample is superconducting. This point will be addressed shortly.

The $LiAl_xTi_{2-x}O_4$ series was prepared as an analogous system to the $Li_{1+x}Ti_{2-x}O_4$ series. The Al^{3+} cations, having no *d* electrons or magnetic moment, should mimic Li^+ substitution at the octahedral sites. The superconducting transition temperature in the aluminum series is nearly constant through $x = 0.2$ (Fig. 2) after which T_c falls gradually to 6.45 K at $x = 0.33$. No superconductivity is observed in the multiphased $x > 0.33$ compositions. A decrease in signal amplitude was observed for increasing x values. The persistence of superconductivity in the $x < 0.33$ compositions is remarkable considering that nearly 17% of the titanium sublattice has been substituted by a foreign cation. The comparison to the $Li_{1+x}Ti_{2-x}O_4$ series is intriguing; T_c, in that system, is constant up to $x = 0.12$, after which superconductivity is suppressed (*6*). This suggests that the precipitous depression of T_c scales with the valence state of the dopant cation, or more formally, with the nominal conduction electron density n_e.

Magnetism

$LiAl_xTi_{2-x}O_4$

The magnetic susceptibilities of the aluminum series were fit to the function

$$\chi_M = (C/T) + \chi_{\text{Pauli}} + A_{\text{TD}}T, \qquad (6)$$

where χ_m is the molar susceptibility, C is the Curie constant, χ_{Pauli} is the temperature-independent term reflecting the Pauli paramagnetism of the conduction electrons, and A_{TD} is a temperature-dependent term similar to that observed in $LiTi_2O_4$ (*4*, *6*). As in the $Li_{1+x}Ti_{2-x}O_4$ and $Li_{1-x}Mg_xTi_2O_4$ series, the $LiAl_xTi_{2-x}O_4$ molar susceptibilities are characterized by small Curie terms, corresponding to approximately 1–2 mole % spin $S = 1/2$ moments, together with substantial χ_{Pauli} and A_{TD} contributions. Representative magnetic suscpetibilities are shown in Fig. 3 and the fit parameters are compiled in Table III.

The χ_{Pauli} term rises rapidly with the addition of a small amount of aluminum ($x <$

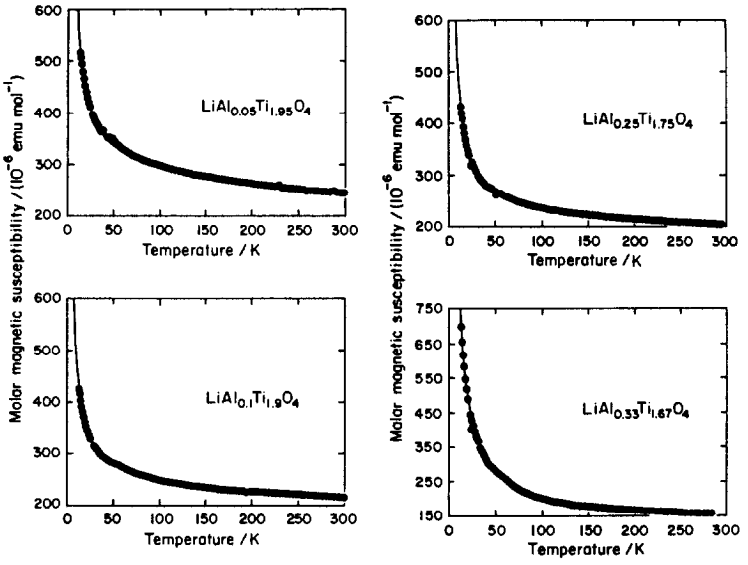

FIG. 3. Magnetic susceptibility data for $LiAl_xTi_{2-x}O_4$ (x = 0.05, 0.10, 0.25, and 0.33).

0.01) and then decreases in a nearly linear fashion through x = 0.33 (Fig. 4). The A_{TD} contribution also exhibits a sharp change in magnitude at low aluminum concentrations and then falls toward zero as x increases (Fig. 4). The two terms appear to be correlated; a similar interdependence is seen in the $Li_{1+x}Ti_{2-x}O_4$ system (*6*).

The decrease in χ_{Pauli} with increasing x values indicates a loss of conduction electron density. In the $Li_{1+x}Ti_{2-x}O_4$ series, the decrease in χ_{Pauli} is well correlated with the location of the metal–nonmetal transition (MNMT) (*6*). Presumably, electrons are localized (and spin-paired) as the material becomes nonmetallic, since a corresponding

TABLE III

MAGNETIC SUSCEPTIBILITY PARAMETERS FOR $LiAl_xTi_{2-x}O_4$

x	Fit temperatures (K)	C	Mole % S = 1/2 (g = 2)	χ_{Pauli} $\times 10^6$ (emu/mole)	A_{TD} $\times 10^6$ (emu/mole)
0.00	12–300	0.00205(2)	0.6	268(1)	−0.146(4)
0.00	12–300	0.00687(5)	1.8	248(2)	−0.138(10)
0.005	12–300	0.00762(5)	2.2	332(2)	−0.241(11)
0.01	12–300	0.00302(3)	0.9	333(1)	−0.285(6)
0.025	12–300	0.00250(1)	0.7	297(1)	−0.180(3)
0.05	12–300	0.00321(2)	0.9	285(1)	−0.180(4)
0.10	12–300	0.00253(1)	0.7	235(1)	−0.104(2)
0.20	12–300	0.00226(1)	0.6	214(1)	−0.102(2)
0.25	12–300	0.00264(1)	0.7	219(1)	−0.085(3)
0.33	12–300	0.00732(3)	2.0	130(1)	0.001(5)

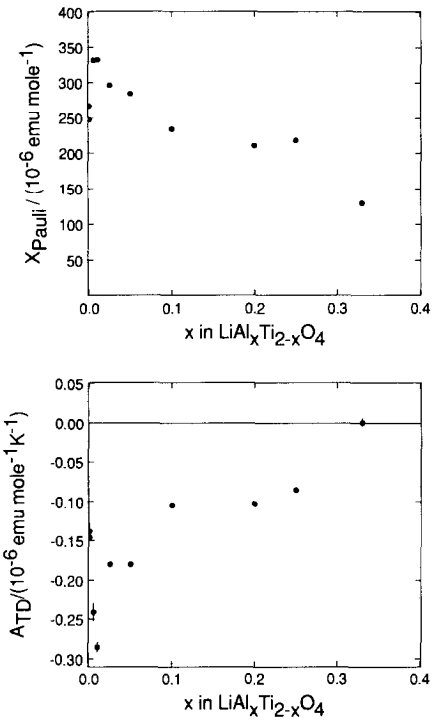

FIG. 4. A The compositional dependence of χ_{Pauli} and A_{TD} for the series $LiAl_xTi_{2-x}O_4$.

surge in Curie behavior is not evident. Unfortunately no conclusive evidence of paired titanium species or clusters in these materials is available, although there is precedent for Ti–Ti dimers in the Magneli phases of Ti_nO_{2n-1} (*21–23*). Additionally, Harrison *et al.* (*24*) have suggested that in the high x value composition of the $Li_{1+x}Ti_{2-x}O_4$ system, both the positive A_{TD} term in the susceptibility and the lineshape of one of two observed ESR absorptions could be due to Ti_2^{6+} and Ti_2^{7+} dimers. Such species may exist as random local phenomena within the structure, or as cooperative lattice distortions. Regardless of the distribution, detection of such clusters by X-ray analysis is difficult in polycrystalline materials.

The A_{TD} contribution to the susceptibility would appear to be related to the actual conduction electron concentration. Presumably, the A_{TD} term corresponds to a temperature-dependent enhancement to the Pauli susceptibility, and is not unexpected in narrow-band materials where electron correlation interactions are important (*24, 25*).

$LiCr_xTi_{2-x}O_4$

As in the $Li_{1-x}Mn_xTi_2O_4$ system (*7*), the χ_{Pauli} and A_{TD} contributions to the magnetic susceptibility are largely obscured in the $LiCr_xTi_{2-x}O_4$ system by the spontaneous paramagnetism associated with Cr^{3+}. Representative susceptibilities are shown in Fig. 5 and the fitted results are given in Table IV.

At low chromium concentrations the Cr^{3+} contribution to the susceptibility is relatively small and the three parameter fit to the experimental data [Eq. (6)] is appropriate. The effective magnetic moments for chromium, calculated from the Curie constant, begin at 4.35 μ_β at $x = 0.0025$. However, at such low chromium concentrations, the Curie contribution from the electrons trapped at oxygen vacancies should also be significant. Assuming an average of 1 mole % vacancies (*7*) the corrected chromium μ_{eff} values are relatively constant at $\sim$ 2.8 μ_β (see Table IV). The χ_{Pauli} and A_{TD} terms obtained for the low doping level chromium samples are of the same magnitude as those for the $LiAl_xTi_{2-x}O_4$ series.

The reduction in the chromium moment from the spin-only Cr^{3+} value of 3.87 μ_β can be attributed to spin exchange interactions with the conduction electrons. If the Cr^{3+} levels are near enough to the Fermi level to interact with the conduction electrons, a reduction in magnetic moment is likely. This reduction would be proportional to $N(E_f)$ and the proximity of the impurity manifold to the Fermi level. A magnetic ion may appear nonmagnetic if the ion lies within the occupied conduction electron states (*25*). The continued presence of a substantial μ_{eff} indicates that the chromium levels are not

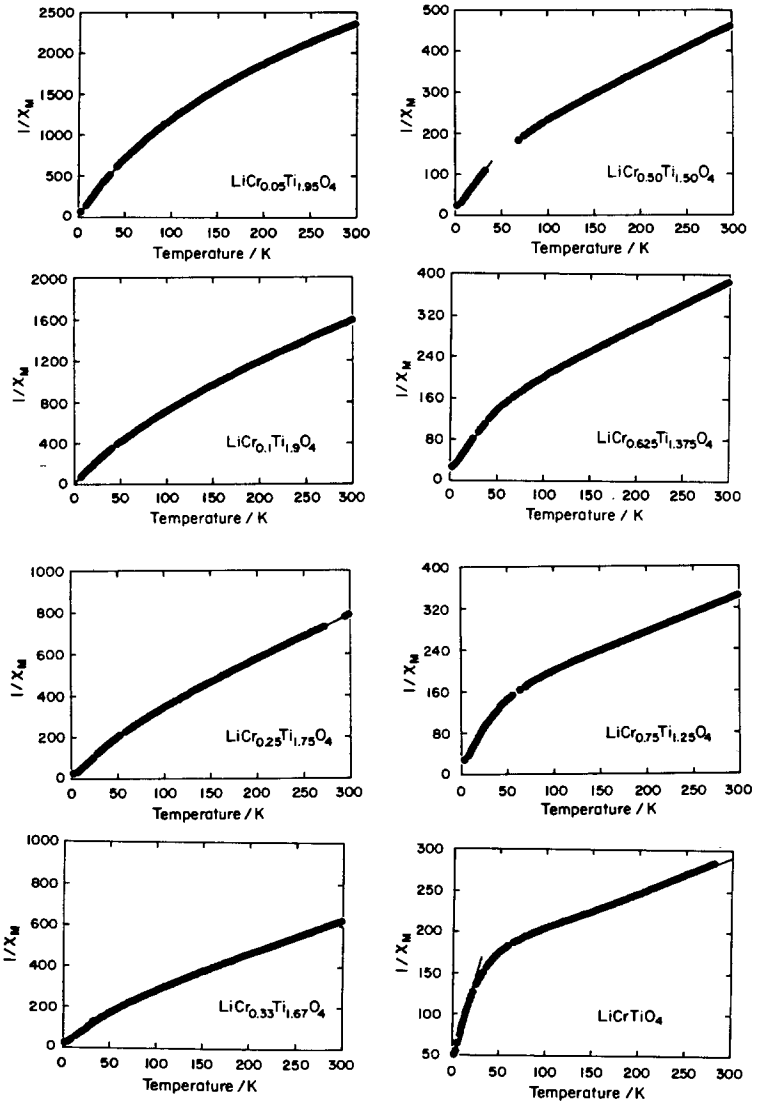

FIG. 5. Plots of reciprocal magnetic susceptibility versus temperature for $LiCr_xTi_{2-x}O_4$, where x = 0.05, 0.10, 0.25, 0.33, 0.50, 0.625, 0.75, and 1.00.

in the conduction electron states, but are near enough to experience a partial reduction in magnetic moment. Theoretically, the change in the magnetic moment as the Fermi level is raised or lowered should indicate the relative location of the chromium levels; a continued reduction in μ_{eff} as x increases would suggest the Cr^3 states are slightly below the conduction band. Unfortunately, such an analysis is limited not only by the uncertainty in the absolute x values at the low chromium concentration, but also by the assumption of a 1 mole % vacancy contribution. Additionally, a wider range of chromium levels is anticipated from the existence of exchange-coupled dimers, tri-

TABLE IV

MAGNETIC SUSCEPTIBILITY PARAMETERS FOR $LiCr_xTi_{2-x}O_4$

x	Fit temperatures (K)	C	μ_{eff} (μ_β)	$-\theta$ (K)	χPauli $\times 10^6$ (emu/mole)	ATD $\times 10^6$ (emu/mole)
	10–300	0.00594(2)	4.35	—	260(1)	−0.154(3)
0.0025			(2.65)[a]			
	10–300	0.00827(2)	3.64	—	249(1)	−0.164(5)
0.005			(2.69)			
	8–300	0.0184(1)	3.13	—	265(4)	−0.21(2)
0.015			(2.80)			
	7—300	0.0363(1)	3.11	—	253(8)	−0.17(5)
0.03			(2.95)			
	9–300	0.0584(1)	3.06	—	250(7)	−0.04(3)
0.05			(2.96)			
	8–300	0.1047(5)	2.89	—	332(33)	−0.08(17)
0.10			(2.84)			
	5–50	0.270(5)	2.94	2.7(2)	—	—
0.25	150–300	0.464(1)	3.85	67.1(6)	—	—
	5–50	0.325(5)	2.79	4.5(2)	—	—
0.33	150–300	0.7157(4)	3.78	83.7(1)	—	—
	5–50	0.349(3)	2.64	4.9(1)	—	—
0.40	150–300	0.7157(4)	3.78	83.7(1)	—	—
	5–50	0.331(2)	2.30	3.4(1)	—	—
0.50	150–300	0.883(1)	3.76	109.2(3)	—	—
	5–50	0.405(3)	2.27	7.0(1)	—	—
0.625	150–300	1.108(1)	3.76	127.1(2)	—	—
	5–50	0.336(4)	1.89	5.1(1)	—	—
0.75	250–300	1.380(1)	3.84	177.8(4)	—	—
	5–25	0.29(1)	1.52	13.0(1)	—	—
1.00	250–300	2.053(8)	4.05	305(2)	—	—

[a] Parentheses indicate μ_{eff} adjusted for 1 mole % S = 1/2 moments.

mers, and larger clusters. In the lower x value compositions, the reciprocal susceptibility is nonlinear throughout the measured temperature range (Fig. 5). However, for the high x value compositions ($x > 0.1$) the reciprocal susceptibility is linear above ~100 K and so can be fit to the inverse Curie–Weiss function. The resulting Curie terms closely match the Cr^{3+} spin-only value of 3.87 μ_β (Fig. 6), implying that the titanium d electrons are either delocalized or spin-paired.

The large negative θ values (shown in Fig. 7) indicate strong antiferromagnetic interactions, as would be expected from direct

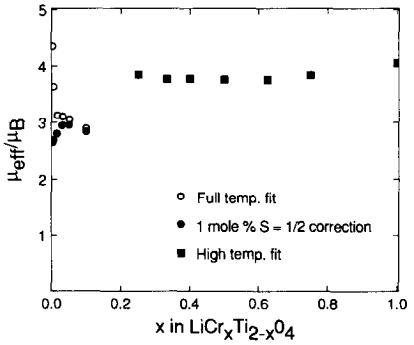

FIG. 6. The effective magnetic moment, μ_{eff} as a function of x for $LiCr_xTi_{2-x}O_4$ (see text for details of temperature ranges used in deriving μ_{eff}).

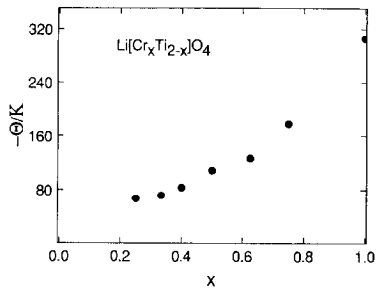

FIG. 7. High temperature θ values for $LiCr_xTi_{2-x}O_4$ ($x > 0.25$).

Cr^{3+}–Cr^{3+} interactions (*25, 26*). The increase in θ with x follows from an increasing exchange energy brought about through a decreasing Cr^{3+}–Cr^{3+} atomic separation and an increase in the overall number of Cr^{3+}–Cr^{3+} interactions as the titanium cation concentration is decreased.

Although the nearest-neighbor magnetic percolation threshold is $x \approx 0.8$ (*26*) for the octahedral sublattice and despite the existence of strong antiferromagnetic exchange interactions, no evidence of magnetic ordering is observed in the concentrated chromium samples. The absence of magnetic ordering may be attributable to the "frustration" inherent to this B sublattice (*27*). Anderson pointed out that the topology of the octahedral sublattice could not support long range order through nearest-neighbor exchange interactions alone (*28*). The presence of predominately antiferromagnetic B–B interactions leads to topological frustration; not all such interactions within a tetrahedron of octahedral sites can be simultaneously satisfied (*27*). Spin frustration may also follow from competing nearest-neighbor and next-nearest-neighbor exchange interactions (*29, 30*) or from the competing interactions of different cations (*31*) and is often expressed as spin-glass behavior. For example, in the spinel series $Zn[Cr_xGa_{2-x}]O_4$, topological frustration leads to spin-glass behavior below 4 K for $0.8 < x < 1.7$ (*32*). Thus, the $LiCr_xTi_{2-x}O_4$ series is a potential spin-glass system. However, since the randomly ordered spin-glass state is usually destroyed by moderate magnetic fields, such behavior may be modified at the field strengths applied in this study or ordering may occur at lower temperatures. Indirect evidence of spin-glass-like behavior has been observed in electron spin resonance studies (*8*).

Although the high temperature regions of the magnetic susceptibilities for $x > 0.1$ are compatible with Curie–Weiss behavior, at lower temperatures a significant deviation is observed which cannot be modeled adequately with the addition of a low temperature Curie contribution. Instead, the effect is likely to result from the formation of spin-exchanged clusters. Within such n-atom clusters, the exchange interaction generates states of distinct total spin value,

$$S' = 1/2, 3/2, 5/2 \ldots \quad nS \text{ for half-integral } nS,$$
$$S' = 0, 1, 2, 3, 4 \ldots \quad nS \text{ for integral } nS, \quad (7)$$

separated by energy gaps proportional to the exchange coefficient J. At temperatures much greater than J/k_B the S' levels are nearly equally occupied and the susceptibility is close to that expected for the isolated ion. At lower temperatures, where $k_BT < J$, only the lower S' levels are occupied. A classic example of exchange-coupled cluster formation is that of $Cr_3(CH_3COO)_6(OH)2Cl \cdot 8H_2O$, where a clear distinction between the $S' = 3/2$ and $S' = 1/2$ regimes is observed in the reciprocal susceptibility (*33, 34*).

The $x > 0.25$ chromium compositions exhibit similar behavior. A reduction in the effective magnetic moment occurs at low temperature as evidenced by the μ_{eff} values calculated from the nearly linear portions of the low temperature reciprocal susceptibility (Table IV). A distribution of cluster sizes

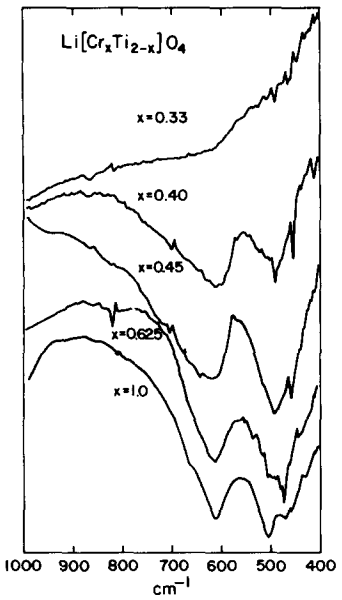

FIG. 8. Infrared transmission spectra (room temperature) for the series $LiCr_xTi_{2-x}O_4$.

and the presence of isolated Cr^{3+} ions contribute in a complicated manner to the observed susceptibility.

Baltzer and Lapatin (*35*) reported a molar Curie constant of 1.35 (corresponding to $\mu_{eff} = 3.29\ \mu_\beta$) and a θ value of -81 K for $LiCrTiO_4$ in the 300–1000 K temperature range. In this study, the Curie constant and value of $LiCrTiO_4$ are 2.3 θ ($\mu_{eff} = 4.32\ \mu_\beta$) and -377 K. However, between 275 and 300 K the reciprocal susceptibility approaches that observed by Baltzer and Lapatin.

Infrared Spectra

The transmission infrared spectra of the $x < 0.4$ compositions of the $LiCr_xTi_{2-x}O_4$ system are characterized by a featureless continuum band absorption associated with delocalized *d* electrons. Vibrational structure is clearly evident in the compositions of $x \geq 0.4$ (Fig. 8).

Reuter and Muller used the value of the Seebeck coefficient to locate the metal-insulator transition in $Mg_{1-x}Li_xV_2O_4$ and $Zn_{1-x}Li_xV_2O_4$ (*36*). Both critical compositions correlated with the appearance of vibrational absorption bands in the IR region. Arndt *et al.* also correlated a metal–insulator transition with the evolution from a continuum absorption to a vibrational spectrum in the IR region (*37*).

Ganguly and Vasanthacharya (*38*) have recently reported infrared spectroscopic studies of the MNMT in perovskites $LaNi_{1-x}B_xO_3$ (B = Cr, Fe and Co). The authors note a disappearance of the vibrational features in the infrared spectra when solid solution composition approaches the region of metallic behavior.

We believe that in the $LiCr_xTi_{2-x}O_4$ system the observed change in the IR region from continuum band absorption to vibrational structure to be indicative of a MNMT in the composition range of $0.33 < x < 0.40$.

In the $LiAl_xTi_{2-x}O_4$ series vibrational absorptions are evident in the $x = 0.25$ and 0.33 compositions (Fig. 9), although in both compositions the absorbing region is broad and appears to be superimposed upon the continuum absorption. In the multiphased higher x value compositions, the vibrational absorptions increase in intensity and resolution, and match the spectrum of ordered

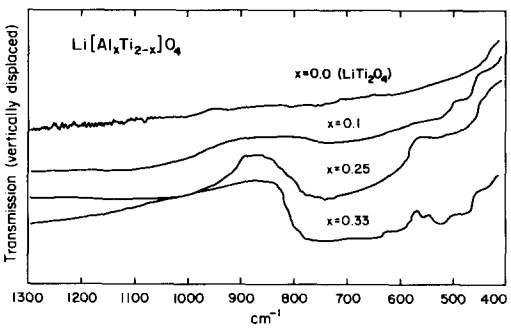

FIG. 9. Infrared transmission spectra (room temperature) for the series $LiAl_xTi_{2-x}O_4$.

$LiAl_5O_8$ (*39*). This impurity phase is easily observed in the higher x value compositions by X-ray diffraction but is not obvious in the lower x value materials. The detection of $LiAl_5O_8$ by X-rays is complicated by the overlap of several diffraction lines with those of the $LiAl_xTi_{2-x}O_4$ series.

Thus the compositions $x = 0.25$ and 0.33 appear to contain two phases; one which is metallic with a conduction-electron absorption, and the $LiAl_5O_8$ impurity phase with strong vibrational absorptions.

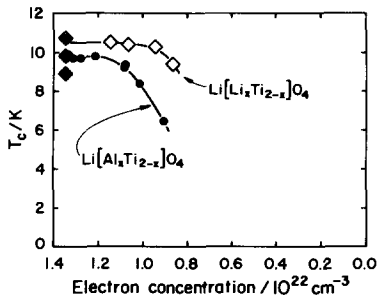

FIG. 10. The superconducting transition temperature, T_c versus nominal electron concentration (n_e) for $Li_{1+x}Ti_{2-x}O_4$ (*6*) and $LiAl_xTi_{2-x}O_4$.

Superconductivity and The Metal-Nonmetal Transition in $LiM_xTi_{2-x}O_4$; $M = Li^+, Al^{3+}, Cr^{3+}$

In this section we outline certain of the major features associated with the compositionally induced MNMT in the title system. As in most systems which span the transition region between localized and itinerant electron states, the questions of electron screening, electron correlation, and disorder are inextricably mixed.

In the $Li_{1-x}Ti_{2-x}O_4$ systems, the MNMT occurs at a considerably reduced x value (~0.1) as compared to that in the corresponding $LiAl_xTi_{2-x}O_4$ ($x > 0.33$) and $LiCr_xTi_{2-x}O_4$ ($x \approx 0.3$–0.4) systems. This situation arises from the relative effects of M^{3+} versus Li^+ substitution on the conduction electron density. In the case of the monovalent substituent ion, the conduction band is drained of electrons three times as rapidly.

However, the $LiAl_xTi_{2-x}O_4$ system bears a strong resemblance to the $Li_{1+x}Ti_{2-x}O_4$ system when the physical properties of each system are scaled to the nominal conduction electron density, n_e, defined as the density of titanium 3*d* electrons (3*d* e^-/cm^3). This quantity effectively normalizes the x values in each system by compensating for the valence difference between Li^+ and Al^{3+}. As examples, we show in Fig. 10 the trend in T_c with n_e for both systems, and in Fig. 11 the variation of χ_{Pauli} and A_{TD} with n_e for each system.

Within and between each series, the trends in T_C, χ_{Pauli}, and A_{TD} are similar when the differences in conduction electron den-

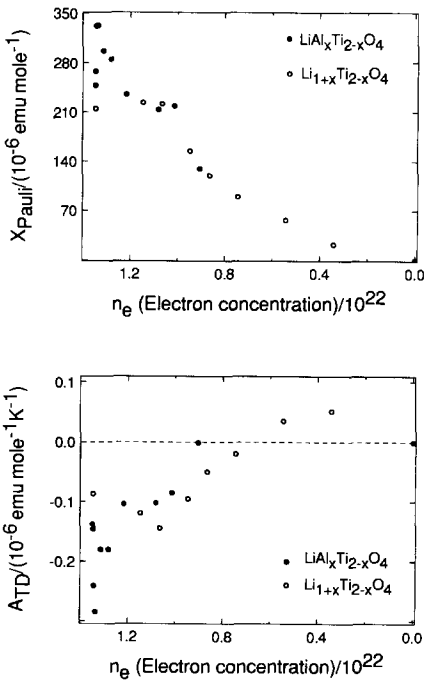

FIG. 11. The compositional dependence of the contributions χ_{Pauli} and A_{TD} to the total magnetic susceptibility, plotted as a function of the nominal electron concentration for $Li_{1+x}Ti_{2-x}O_4$ (*6*) and $LiAl_xTi_{2-x}O_4$.

TABLE V

METAL–NONMETAL TRANSITION IN $LiM_xTi_{2-x}O_4$ (M = Li, Cr, Al).

System	x_c	$n_e \times 10^{21}$
$Li_{1+x}Ti_{2-x}O_4$	~0.12	~8.6
$LiAl_xTi_{2-x}O_4$	≥0.33	~8.9
$LiCr_xTi_{2-x}O_4$	0.33–0.40	~8.6

sity are taken into account. The compositions for which χ_{Pauli} and A_{TD} values are reported in the $Li_{1+x}Ti_{2-x}O_4$ series do not cover the low level substitution region where sharp peaking in these terms is observed in the aluminum series. However, Harrison and Edwards (*40*) did observe an anomalously large χ_{Pauli} value for an x = 0.02 sample. The comparison to the $Li_{1+x}Ti_{2-x}O_4$ system, where the MNMT is positioned at $0.1 < x < 0.15$ (*24*), additionally suggests that a MNMT occurs at a composition near or slightly beyond x = 0.33 in $LiAl_xTi_{2-x}O_4$ and that a common or analogous mechanism may drive the MNMT in both these series.

The infrared transmission result for the $LiCr_xTi_{2-x}O_4$ series describes the rapid evolution from the metallic to nonmetallic behavior at $0.33 < x < 0.40$ and a nominal electron density, n_e of 8.6×10^{21} cm^{-1}. Thus, the MNMT for each of the $LiM_xTi_{2-x}O_4$ ($M = Li^+, Al^{3+}, Cr^{3+}$) systems occurs at virtually the same n_e value (Table V). Clearly, T_c variation in the $Li_{1+x}Ti_{2-x}O_4$ is dominated by the magnetic effects and x_c cannot be estimated from this compositional behavior.

The peculiar T_c trend observed in the aluminum and lithium series is difficult to rationalize in terms of the BCS theory of superconductivity (*41*). A variation in T_c with changing n_e would be anticipated in sharp contrast to the observed persistence of a high T_c across quite a large homogeneity range in x. In the absence of a satisfactory explanation for the T_c behavior, microscopic chemical inhomogeneities have been considered (*24*). In the most obvious picture, a bulk disproportionation occurs with superconducting $LiTi_2O_4$ as one product. The concentration of this superconducting phase then decreases as the nominal composition is adjusted toward the insulating endmember. The T_c would remain constant and the superconducting volume fraction would then decrease linearly with x, as is observed experimentally (*24*).

The apparent homogeneity on a X-ray wavelength scale sets the upper limit to any homogeneity fluctuations of ca. 500 Å in these materials, and the calculated superconducting coherence length of approximately 26 Å represents the lower limit (*24*). Segregation on such a fine scale is indicative of spinodal decomposition (*42, 43*). As opposed to the nucleation and growth mechanism of disproportionation in which the second phase is fairly localized and of constant composition, the spinodal decomposition is characterized by a continuous change in the compositions of the disproportionating phases. As a result, the homogeneity fluc-

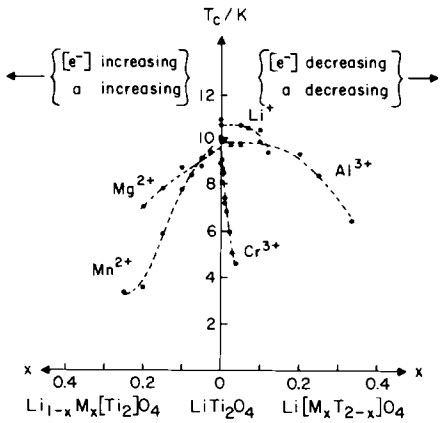

FIG. 12. The substitutional chemistry of $LiTi_2O_4$. The compositional dependence of cation-substituted $LiTi_2O_4$ including $Li_{1-x}M_xTi_2O_4$ (*7*) and $LiM_xTi_{2-x}O_4$ (present investigation). A-site cation substitution ($Li_{1-x}M_xTi_2O_4$) increases both a and n_e; B-site cation substitution ($LiM_xTi_{2-x}O_4$) decreases both a and n_e.

tuations are slight and finely segregated with a high degree of connectivity.

The transmission infrared spectra of the $LiAl_xTi_{2-x}O_4$ series show the presence of insulating phases in compositions on the metallic side of the MNMT, and so demonstrate some consistency with the disproportionation model. However, samples of composition $x = 0.025$ and 0.075 in the $Li_{1+x}Ti_{2-x}O_4$ series were subsequently prepared to check for similar insulating phases by IR. No vibrational absorptions were observed in either composition.

In addition, direct evidence of disproportionation has not been found in prelmininary high resolution electron microscopy (HREM) studies. Examination of the $LiAl_{0.33}Ti_{1.67}O_4$ composition has revealed a majority phase with an electron diffraction pattern consistent with the spinel space group, and two minority phases which were not found in sufficient crystallinity for electron diffraction. However, qualitative characterization of the two minority phases suggests, respectively, a spinel with superstructure, and a highly disordered, poorly crystalline material. The former material is undoubtedly the ordered $LiAl_5O_8$ impurity phase which is known to exhibit a superstructure of ordered cations (*44*), and the latter phase is most likely the unidentified and nonsuperconducting impurity phase (*6, 16*). within the majority phase no evidence of intergrowth or composition fluctuation is present.

The disproportionation scenario, even on the 25 Å scale, should alter the MNMT mechanism. rather than percolation along discrete sites of the octahedral sublattice in a compositionally homogeneous system, percolation between the disproportionation phases (at least one of which is superconducting) dictates the position of the mnmt, and the T_c dependence. Continuum percolation is characterized by topological disorder, and the critical percolation threshold is defined in terms of a critical volume fraction (*45*). Conveniently, the critical threshold dependence upon lattice type is immaterial in continuum percolation, and both the theoretical and empirical results place the critical percolation volume at ca. 16% (*45, 46*).

Presumably, a MNMT could then occur in a range of x values depending upon the extent of the spinodal decomposition and the volume occupation of the resulting phases. The superconducting transition temperature would be dependent upon the tunneling probability between the superconducting regimes, which again would be determined by the nature of the decomposition. Recent studies have presented results supporting bulk superconductivity in the $Li_{1+x}Ti_{2-x}O_4$ system (*47,48*). The observed decrease in the superconducting volume fraction is explained as a percolative restriction of the superconducting pairs to a decreasing volume fraction of a chemically homogeneous crystallite. A classical percolation interpretation of superconductivity and the MNMT in the $LiM_xTi_{2-x}O_4$ systems has been previously presented by Lambert *et al.* (49).

Concluding Remarks

The physical properties of the $Li_{1+x}Ti_{2-x}O_4$ series have been extensively studied, yet a comprehensive understanding of these properties and the MNMT is lacking. The existence of compositional inhomogeneities remains unconfirmed and their possible significance undetermined. As an further example of the gaps in our current understanding of these systems we note the important question of oxygen vacancies. The presence of oxygen vacancies within the materials has been well established by magnetic susceptibility and electron spin resonance investigations (*5, 6*). However, the corresponding relationship between the concentration of these centers and the superconducting volume fraction is uncertain (*50*).

The polycrystalline nature of the $Li_{1+x}Ti_{2-x}O_4$ materials undoubtably contributes to such puzzling physical properties. However, the intricacies of the system may not be resolved by the synthesis of single crystals since such crystals may be intrinsically different, particularly if nonstoichiometry and inhomogeneity influence the properties of the powder samples. The preparation of analogous powder series, such as $LiCr_xTi_{2-x}O_4$ and $LiAl_xTi_{2-x}O_4$ provides a possible alternative approach to the understanding of the $Li_{1+x}Ti_{2-x}O_4$ system.

One overriding feature which emerges from the studies on cation-substituted $LiTi_2O_4$ is the proximity of the parent compound to the MNMT. In Fig. 11 we have attempted to highlight this feature; increasing or decreasing the electron density in cation-substituted $LiTi_2O_4$ serves always to reduce T_c from the value of ca. 11 K. The ability to synthesize oxides close to the MNMT region will always raise the possibility of high temperature superconductivity (*51*).

Acknowledgments

We thank Sandra Issler for the powder diffractometer measurements and D. A. Jefferson of Cambridge University for the HREM results. This research was sponsored by the Air Force Office of Scientific Research, NSF, SERC(UK), the Material Science Centre at Cornell University, and British Petroleum (VRU and EMRA Awards), P.M.L. also acknowledges an ARCO Doctoral Fellowship.

References

1. A. Deschanvres, B. Raveau, and Z. Sekkal, *Mater. Res. Bull.* **6,** 699 (1971).
2. D. C. Johnston, H. Prakash, W. H. Zachariasen, and R. Viswanathan, *Mater. Res. Bull.* **8,** 777 (1973).
3. D. C. Johnston, Ph.D. Thesis, University of California, San Diego (1975).
4. D. C. Johnston, *J. Low Temp. Phys.* **25,** 145 (1976).
5. M. R. Harrison, D. Phil. Thesis, Oxford University (1981).
6. M. R. Harrison, P. P. Edwards, and J. B. Goodenough, *J. Solid State Chem.* **54,** 136 (1984).
7. P. M. Lambert, M. R. Harrison, and P. P. Edwards, *J. Solid State Chem.*, **75,** 332 (1988).
8. P. M. Lambert, Ph.D. Thesis, Cornell University (1986).
9. H. Furuhashi, M. Inagaki, and S. Naka, *J. Inorg. Nucl. Chem.* **35,** 3009 (1973).
10. K. Yvon, W. Jeitschko, and E. Parte, *J. Appl. Crystallogr.* **10,** 73 (1977).
11. D. C. Johnson, Ph.D. Thesis, Cornell University (1983).
12. H. P. R. Frederikse and G. A. Canela, *Phys. Rev.* **147,** 583 (1966).
13. F. E. Senftle and A. N. Thorpe, *Phys. Rev.* **175,** 1144 (1968).
14. E. Kordes and E. Rottig, *Z. Anorg. Allegem. Chem.* **264,** 34 (1951).
15. G. Blasse, *Philips Res. Rep. Suppl* **3,** (1964).
16. T. Inukai and T. Murakami, *Japan J. Appl. Phys.* **22,** (Suppl. 22–2), 61 (1983).
17. B. Morosin and J. C. Mikkelson, *Acta Crystallogr.* **B25,** 798 (1979).
18. G. Blasse, *J. Inorg. Nucl. Chem.* **25,** 230 (1963).
19. A. A. Abrikosov and L. P. Gor'kov, *Sov. Phys. JETP,* **12,** 1243 (1961).
20. M. B. Maple, *in* "Magnetism," (G. T. Rado and H. Suhl, Eds.), Vol. V, Academic Press, New York, 289 (1973).
21. J. F. Houlihan, W. J. Danley, and L. N. Mulay, *J. Solid State Chem.* **12,** 265 (1975).
22. S. A. Fairhurst, A. D. Inglis, Y. LePage, J. R. Morton, and K. F. Preston, *Chem. Phys. Lett.* **95,** 444 (1983).
23. S. A. Fairhurst, A. D. Inglis, Y. LePage, J. R. Morton, and K. F. Preston, *J. Magn. Reson.* **54,** 300 (1983).
24. M. R. Harrison, P. P. Edwards, and J. B. Goodenough, *Phil Mag. B.* **52,** 679 (1985).
25. C. M. Hurd, "Electrons in Metals," Wiley, New York, pp. 42–144 (1975).
26. J. B. Goodenough, *Phys. Rev.* **117,** 1442 (1960).
27. D. Fiorani, L. Gastaldi, A. Lapiccirella, 5. Viticolo, and N. Tomassini, *Solid State Commun.* **32,** 831 (1979).
28. P. W. Anderson, *Phys. Rev.* **102,** 1008 (1956).
29. J. Villian, *Z. Physik.* **B33,** 31 (1979).
30. M. Alba, J. Hammann, and M. Nogues, *J. Phys.* **C15,** 5441 (1982).
31. D. Fiorani, M. Nogues and S. Viticoii, *Solid State Comm.*, **41,** 537 (1982).
32. H. Maletta and W. Felsch, *Phys. Rev.*, **B20,** 1245 (1979).
33. D. Fiorani, S. Viticoli, J. L. Dormann, J. L. Tholence, J. Hammann, A. P. Murani, and

J. L. SOUBEYROUX, *J. Phys.* **C16,** 3175 (1983).

34. J. WUCHER AND H. M. GIJSMAN, *Physica* **20,** 361 (1954).
35. P. K. BALTZER AND E. LAPATIN, "Proceedings of the International Conference on Magnetism," Nottingham, 564 (1964).
36. B. REUTER AND K. MÜLLER *Naturwissenschaflern* **54,** 164 (1967).
37. D. ARNDT, K. MÜLLER, B. REUTER, AND E. REIDEL, *J. Solid State Chem.* **10,** 270 (1974).
38. P. GANGULY AND N. Y. VASANTHACHARYA, *J. Solid State Chem.* **61,** 164 (1980).
39. S. HAFNER AND F. LAVES, *Z. Kristallogr.* **115,** 331 (1964).
40. M. R. HARRISON AND P. P. EDWARDS, unpublished observations.
41. J. BARDEEN, L. N. COOPER, AND J. R. SCHRIEFFER, *Phys. Rev.* **108,** 1175 (1957).
42. J. W. CAHN, *J. Chem. Phys.* **42,** 93 (1965).
43. C. N. R. RAO AND K. J. RAO, "Phase Transitions in Solids," McGraw Hill International Book Co., New York, pp. 133–143 (1978).
44. R. COLLONGUES, *Ann. Chimie* **8,** 395 (1963).
45. R. ZALLEN, "The Physics of Amorphous Solids," Wiley, New York (1983).
46. I. WEBMAN, J. JORTNER, AND M. H. COHEN, *Phys. Rev.,* **B14,** 4737 (1976).
47. Y. UEDA, T. TANAKA, K. KOSUGE, M. ISHIKAWA, AND H. YASUOKA, *J. Solid State Chem.* **77,** 401 (1988).
48. M. ITOH, Y. HASEGAWA, I. YAMADA, H. YASUOKA, Y. UEDA, AND K. KOSUGE, *J. Phys. Soc. Japan,* in press.
49. P. M. LAMBERT, M. R. HARRISON, D. E. LOGAN, AND P. P. EDWARDS, "Disordered Semiconductors" (M. A. Kastner, G.A. Thomas, and S. R. Orshinsky, Eds.), Plenum, New York, p. 135 (1987).
50. D. W. MURPHY, M. GREENBLATT, S. M. ZAHURAK, R. J. CAVA. J. V. WASZCZAK, G. W. HULL, AND R. S. HUTTON, *Rev. Chim. Miner.* **19,** 441 (1982).
51. G. BEDNORZ AND K. A. MULLER, *Z. Phys.* **B64,** 189 (1986).